

A Knee Modular Orthosis Design Based on Kinematic Considerations

C. Copilusi, C. Ploscaru

Abstract—This paper addresses attention to a research regarding the design of a knee orthosis in a modular form used on children walking rehabilitation. This research is focused on the human lower limb kinematic analysis which will be used as input data on virtual simulations and prototype validation. From this analysis, important data will be obtained and used as input for virtual simulations of the knee modular orthosis. Thus, a knee orthosis concept was obtained and validated through virtual simulations by using MSC Adams software. Based on the obtained results, the modular orthosis prototype will be manufactured and presented in this article.

Keywords—Human lower limb, children orthoses, kinematic analysis, knee orthosis.

I. INTRODUCTION

HUMAN rehabilitation got a lot of progress due to the modern research technology and techniques. A major impact on this research domain was given by the robotic systems implementation on daily activities under rehabilitation or recovery programs. As an example of positive results, it can be remarked on the human walking rehabilitation research, where a large variety of prosthesis and orthotic systems have been designed and manufactured. By considering a particular area of these, which regards the orthotic systems for human lower limb rehabilitation, many orthotic systems have been designed mainly for adults or elderly persons. In case of children, these particular systems are extremely rare due to the fact that a child is in a continuous growth. Basically, specific companies and research centers need to develop parameterized models for any child's age and anthropomorphic data. On this research area, it can be identified prototypes like: An active knee orthotic device from [1], an ankle foot orthosis from [2], NEDO Project in [3], smart prosthesis in [4] and a rehabilitation device with intelligent control in [5]. Also, those concepts were designed by taking into account kinematic considerations. Similar kinematic analyses, with remarkable results, can be found in [9]-[11]. Regarding these analyses, orthotic systems can be developed on a modular form in order to improve the locomotion system and to satisfy the ability to move in case of children with ages between 4 to 7 years old.

A first starting point on this research frame is represented by a state-of-the-art with kinematic analyses performed by other researchers. Some rehabilitation solutions especially designed for children have been studied; mainly active

orthoses as the one for a child ankle joint shown on [6] and a powered knee orthosis design from [7].

In order to develop and perform a kinematic analysis of the human lower limb, it is necessary to choose the desired method for study the entire human lower limb kinematic model. The general method used in kinematic analysis was reported in [8], where the algorithm was considered as a starting point. For this, on the second section, a general kinematic method is described with application on mobile systems analysis especially mechanical ones. By taking into account this method, a kinematic model of the human lower limb was elaborated with proper kinematic equations in third section. This kinematic model is a parameterized one and through a computational calculus, important data were obtained for virtual simulations of the modular orthosis prototype. Thus, in fourth section, virtual simulations of a knee modular orthosis concept were performed with the aid of MSC Adams software. These were performed by using similar input data regarding the contact in mechanics, which was reported in [13]. This was achieved by using kinematic data as input parameters. In this way, the presented orthosis concept was validated and a real model was fabricated, according with specialty literature data from [12], where only the knee angular amplitude was considered as reference point for validating the knee orthosis design.

Based on the obtained prototype and analysis results, important data were synthesized on the final conclusions of this research.

II. KINEMATIC METHOD DESCRIPTION

The method used on this research is characterized by flexibility due to an interface for dynamic analysis especially for finite element modeling of spatial and planar mobile mechanical systems as in [8].

A. Mathematic Model

The general kinematic algorithm which will be adapted for the human lower limb mathematic model is characterized by "n" solid rigid bodies connected together through "n-1" kinematic pairs as it can be remarked on Fig. 1. For this, the following notations will be made: $T_i(x_i, y_i, z_i)$ represents the reference coordinate system attached to "i" element, having $\overline{W}_i(\overline{i}_i, \overline{j}_i, \overline{k}_i)$ versors base with $i = \overline{1, n}$; $T_0(x_0, y_0, z_0)$ represents the global reference system with $\overline{W}_0(\overline{i}_0, \overline{j}_0, \overline{k}_0)$ versors base; $\overline{\delta}_i$ represents the relative translation vector between "i-1" and "i" elements, depending with T_{i-1} tried, if

C. Copilusi is with the Faculty of Mechanics, University of Craiova. Calea Bucuresti street, no. 107. Romania (corresponding author to provide phone: +4 0747222771; e-mail: cristache03@yahoo.co.uk).

C. Ploscaru is with Faculty of Mechanics, University of Craiova. Calea Bucuresti street no. 107. Romania (e-mail: ccploscaru@yahoo.ro).

exists a translation joint between “ $i-1$ ” and “ i ”, ($i = \overline{1, n}$); \bar{r}_i represents the position vector which depends with \bar{T}_{i-1} , reference system, against with O_{i-1} , point, when the relative translation starts ($i = \overline{1, n}$); \bar{S}_i represent the position vector of the M_i , depending with T_i , attached to “ i ” element.

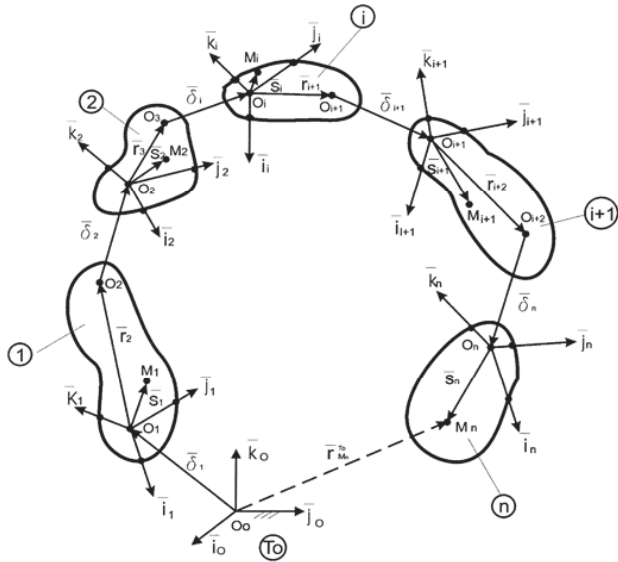


Fig. 1 Kinematic model created from “ n ” solid rigid bodies connected together through “ $n-1$ ” kinematic joints

B. Position Kinematic Analysis

The position vector of “ M_n ” point, depending on the global reference system is given by:

$$\bar{r}_{Mn}^{T0} = \overline{O_0M_n} = \sum_{i=1}^n (\bar{r}_i + \bar{\delta}_i) + \bar{S}_n \tag{1}$$

where:

$$\bar{r}_i = \{r_i^x, r_i^y, r_i^z\}^T_{i-1} = \{r_i\}^T \{ \bar{W}_{i-1} \} \tag{2}$$

$$\bar{\delta}_i = \{\delta_i^x, \delta_i^y, \delta_i^z\}^T_{i-1} = \{\delta_i\}^T \{ \bar{W}_{i-1} \} \tag{3}$$

$$\bar{S}_n = \{S_n^x, S_n^y, S_n^z\}^T_{i-1} = \{S_n\}^T \{ \bar{W}_n \} \tag{4}$$

Also the following connection order will be considered:

$$0 - 1 - 2 - 3 - \dots - i-1 - i \dots n$$

The transformation coordinates matrix will be introduced, in order to cross from a reference coordinate system to another:

$$\{ \bar{W}_{i-1} \} = [A_{0,i-1}] \cdot \{ \bar{W}_0 \} \tag{5}$$

Thus, (2), (3) and (4) become:

$$\bar{r}_i = \{r_i\}^T \{ \bar{W}_{i-1} \} = \{r_i\}^T [A_{0,i-1}] \{ \bar{W}_0 \} \tag{6}$$

$$\bar{\delta}_i = \{\delta_i\}^T \{ \bar{W}_{i-1} \} = \{\delta_i\}^T [A_{0,i-1}] \{ \bar{W}_0 \} \tag{7}$$

$$\bar{S}_n = \{S_n\}^T \{ \bar{W}_{i-1} \} = \{S_n\}^T [A_{0,n}] \{ \bar{W}_0 \} \tag{8}$$

By introducing (6)-(8) in (1), the final position calculus will be obtained:

$$\bar{r}_{Mn}^{T0} = \overline{O_0M_n} = \sum_{i=1}^n \left(\left(\{r_i\}^T + \{\delta_i\}^T \cdot [A_{0,i-1}] \right) + \{S_n\}^T \cdot [A_{0,n}] \right) \cdot \{ \bar{W}_0 \} \tag{9}$$

C. Velocity Kinematic Analysis

Velocities will be processed by differentiating (9) by taking into account time as parameter. Considering the coordinates transformation matrix as a quadratic one, it will be written:

$$[A_{0i}] \cdot [A_{0i}]^T = [I] \tag{10}$$

By differentiating (10) depending on time, the mathematical expression will be obtained:

$$[\dot{A}_{0i}] \cdot [A_{0i}]^T + [A_{0i}] \cdot [\dot{A}_{0i}]^T = 0 \tag{11}$$

$$\left[[\dot{A}_{0i}] \cdot [A_{0i}^T] \right]^T = [A_{0i}] \cdot [\dot{A}_{0i}]^T = - [\dot{A}_{0i}] \cdot [A_{0i}]^T \tag{12}$$

From (11) can be remarked that $[\dot{A}_{0i}] \cdot [A_{0i}]^T$ - term is a non symmetric matrix:

$$[\tilde{\omega}_{0i}] = [\dot{A}_{0i}] \cdot [A_{0i}]^T \tag{13}$$

By multiplying (13) with $[A_{0i}]$, leads to:

$$[\tilde{\omega}_{0i}] \cdot [A_{0i}] = [\dot{A}_{0i}] \tag{14}$$

Differentiating (14) by taking into account time, it can be written:

$$\dot{\bar{r}}_{Mn}^{T0} = \sum_{i=1}^n \left(\left(\{r_i\}^T \cdot [\tilde{\omega}_{0,i-1}] + \{\delta_i\}^T + \{S_n\}^T \cdot [\tilde{\omega}_{0n}] \right) \cdot [A_{0,i-1}] \right) \cdot \{ \bar{W}_0 \} \tag{15}$$

A non symmetric matrix will be obtained:

$$\left[\tilde{\omega}_{0,p} \right] = \begin{bmatrix} 0 & \omega_{0,p}^z & -\omega_{0,p}^y \\ -\omega_{0,p}^z & 0 & \omega_{0,p}^x \\ \omega_{0,p}^y & -\omega_{0,p}^x & 0 \end{bmatrix} \quad (16)$$

where:

$$\bar{\omega}_{0,p} = \omega_{0,p}^x \bar{i} + \omega_{0,p}^y \bar{j} + \omega_{0,p}^z \bar{k} \quad (17)$$

For each vector $\bar{\delta}_i$, \bar{r}_i and \bar{S}_i , ($i = \bar{1}, n$), a non symmetric matrix can be attached similar to (16). The used terms from (15), can be written onto the following form:

$$\{r_i\}^T \left[\tilde{\omega}_{0,i-1} \right] = \{\omega_{0,i-1}\}^T \left[\tilde{r}_i \right] \quad (18)$$

$$\{\delta_i\}^T \left[\tilde{\omega}_{0,i-1} \right] = \{\omega_{0,i-1}\}^T \left[\tilde{\delta}_i \right] \quad (19)$$

$$\{S_n\}^T \left[\tilde{\omega}_{0,n} \right] = \{\omega_{0,n}\}^T \left[\tilde{S}_n \right] \quad (20)$$

$$\{\omega_{op}\} = \{\omega_p^x, \omega_p^y, \omega_p^z\} \quad (21)$$

By considering the above mathematical expressions, (15) can be written:

$$\begin{aligned} \bar{V}_{Mn}^{T_0} &= \left(\begin{aligned} &\sum_{i=1}^n \left(\{\omega_{0,i-1}\}^T \left[\tilde{r}_i \right] + \right. \\ &+ \left. \{\omega_{0,i-1}\}^T \left[\tilde{\delta}_i \right] \right) \cdot [A_{0,i-1}] + \\ &+ \sum_{i=1}^n [A_{0,i-1}]^T \left[\dot{\tilde{\delta}}_i \right] + \\ &+ \left. \{\omega_{0,n}\}^T \left[\tilde{S}_n \right] \cdot [A_{0,n}] \right) \cdot \{\bar{W}_0\} = \\ &= \left(\begin{aligned} &\sum_{i=1}^n \left(\{\omega_{0,i-1}\}^T \left[\tilde{r}_i \right] \cdot [A_{0,i-1}] + \right. \\ &+ \sum \left. \left[\dot{\tilde{\delta}}_i \right]^T \cdot [A_{0,i-1}] + \right. \\ &+ \sum_{i=1}^n \left. \left. \{\omega_{0,i-1}\}^T \left[\tilde{\delta}_i \right] \cdot [A_{0,i-1}] + \right. \right. \\ &+ \left. \left. \{\omega_{0,n}\}^T \left[\tilde{S}_n \right] \cdot [A_{0,n}] \right) \right) \cdot \{\bar{W}_0\} \end{aligned} \right) \quad (22) \end{aligned}$$

D. Accelerations Kinematic Analysis

The accelerations mathematical expressions can be obtained by differentiating (22) depending on time in a similar procedure as the velocities.

III. HUMAN LOWER LIMB KINEMATIC ANALYSIS

By considering the anatomical model of a human lower limb, 3 main joints can be identified. Also, by taking into account the main motions of this, it can be identified a number of 8 motions, which corresponds with 8 joints. Thus, a human lower limb simplified kinematic model is shown in Fig. 2. Therefore, a kinematic analysis will be performed only for walking activity, in case of a single gait. The kinematic parameters variation laws were obtained by processing with the MAPLE software a parameterized mathematical model of a child with an age of 7 years old and this defines the human lower limb experimental kinematic analysis.

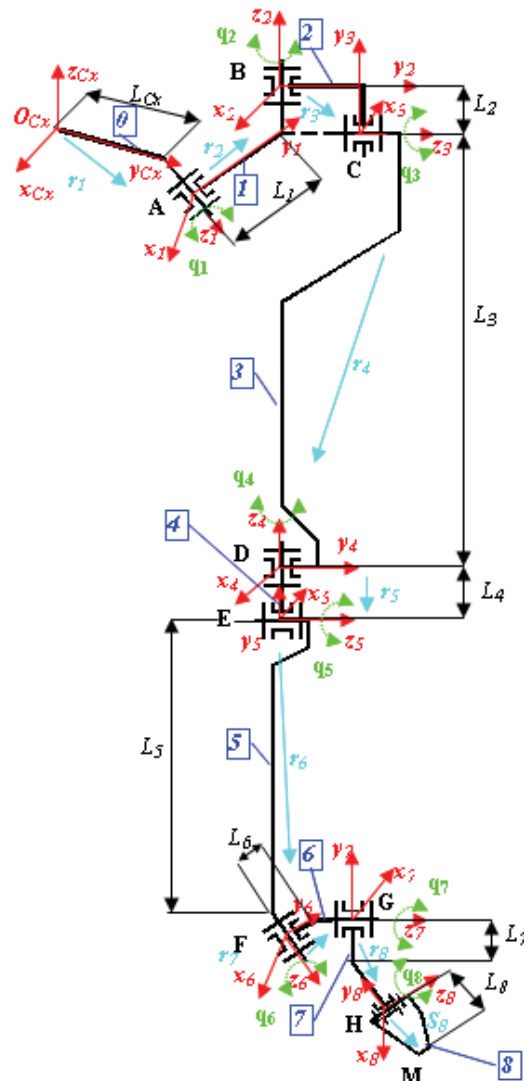


Fig. 2 A simplified kinematic model of the human lower limb

From a structural viewpoint, the kinematic linkage consists of 8 rotation joints.

The \bar{r}_i position vectors on T_{i-1} reference coordinate system are:

$$\begin{aligned}
 \mathbf{r}_1 &= [0, L_{cx}, 0]_{cx}^T; \mathbf{r}_3 = [0, 0, -L_2]_2^T; & \{\overline{\mathbf{W}}_1\} &= [A_{Cx1}] \cdot \{\overline{\mathbf{W}}_{Cx}\} & (35) \\
 \mathbf{r}_2 &= [0, L_1, 0]_1^T; \mathbf{r}_4 = [0, -L_3, 0]_3^T; & \{\overline{\mathbf{W}}_2\} &= [A_{12}] \cdot \{\overline{\mathbf{W}}_1\} = [A_{Cx2}] \cdot \{\overline{\mathbf{W}}_{Cx}\} & (36) \\
 \mathbf{r}_5 &= [0, 0, -L_4]_4^T; \mathbf{r}_6 = [0, -L_5, 0]_5^T; & \{\overline{\mathbf{W}}_3\} &= [A_{23}] \cdot \{\overline{\mathbf{W}}_2\} = [A_{Cx3}] \cdot \{\overline{\mathbf{W}}_{Cx}\} & (37) \\
 \mathbf{r}_7 &= [0, L_6, 0]_6^T; \mathbf{r}_8 = [0, -L_7, 0]_7^T; & \{\overline{\mathbf{W}}_4\} &= [A_{34}] \cdot \{\overline{\mathbf{W}}_3\} = [A_{Cx4}] \cdot \{\overline{\mathbf{W}}_{Cx}\} & (38) \\
 \mathbf{S}_8 &= [0, -L_8, 0]_8^T. & \{\overline{\mathbf{W}}_5\} &= [A_{45}] \cdot \{\overline{\mathbf{W}}_4\} = [A_{Cx5}] \cdot \{\overline{\mathbf{W}}_{Cx}\} & (39)
 \end{aligned}
 \tag{23}$$

A connection order will be considered as:

$$C_x - 1 - 2 - 3 - 4 - 5 - 6 - 7 - 8$$

A. Position Analysis

The position vectors are:

$$\overline{\mathbf{r}}_1 = \{r_1^x, r_1^y, r_1^z\} = \{\mathbf{r}_1\}^T \cdot \{\overline{\mathbf{W}}_{Cx}\} \tag{24}$$

$$\overline{\mathbf{r}}_2 = \{r_2^x, r_2^y, r_2^z\} = \{\mathbf{r}_2\}^T \cdot \{\overline{\mathbf{W}}_1\} \tag{25}$$

$$\overline{\mathbf{r}}_3 = \{r_3^x, r_3^y, r_3^z\} = \{\mathbf{r}_3\}^T \cdot \{\overline{\mathbf{W}}_2\} \tag{26}$$

$$\overline{\mathbf{r}}_4 = \{r_4^x, r_4^y, r_4^z\} = \{\mathbf{r}_4\}^T \cdot \{\overline{\mathbf{W}}_3\} \tag{27}$$

$$\overline{\mathbf{r}}_5 = \{r_5^x, r_5^y, r_5^z\} = \{\mathbf{r}_5\}^T \cdot \{\overline{\mathbf{W}}_4\} \tag{28}$$

$$\overline{\mathbf{r}}_6 = \{r_6^x, r_6^y, r_6^z\} = \{\mathbf{r}_6\}^T \cdot \{\overline{\mathbf{W}}_5\} \tag{29}$$

$$\overline{\mathbf{r}}_7 = \{r_7^x, r_7^y, r_7^z\} = \{\mathbf{r}_7\}^T \cdot \{\overline{\mathbf{W}}_6\} \tag{30}$$

$$\overline{\mathbf{r}}_8 = \{r_8^x, r_8^y, r_8^z\} = \{\mathbf{r}_8\}^T \cdot \{\overline{\mathbf{W}}_7\} \tag{31}$$

$$\overline{\mathbf{S}}_8 = \{S_8^x, S_8^y, S_8^z\} = \{\mathbf{S}_8\}^T \cdot \{\overline{\mathbf{W}}_8\} \tag{32}$$

where:

$$\begin{aligned}
 \{\mathbf{r}_1\}^T &= [0, L_{cx}, 0]_{cx}^T; \{\mathbf{r}_2\}^T = [0, L_1, 0]_1^T; \\
 \{\mathbf{r}_3\}^T &= [0, 0, -L_2]_2^T; \{\mathbf{r}_4\}^T = [0, -L_3, 0]_3^T; \\
 \{\mathbf{r}_5\}^T &= [0, 0, -L_4]_4^T; \{\mathbf{r}_6\}^T = [0, -L_5, 0]_5^T; \\
 \{\mathbf{r}_7\}^T &= [0, L_6, 0]_6^T; \{\mathbf{r}_8\}^T = [0, -L_7, 0]_7^T; \\
 \{\mathbf{S}_8\}^T &= [0, -L_8, 0]_8^T.
 \end{aligned}
 \tag{33}$$

The $\overline{\mathbf{r}}_M^{Cx}$ vector has the following expression:

$$\overline{\mathbf{r}}_M^{Cx} = \overline{\mathbf{r}}_1 + \overline{\mathbf{r}}_2 + \overline{\mathbf{r}}_3 + \overline{\mathbf{r}}_4 + \overline{\mathbf{r}}_5 + \overline{\mathbf{r}}_6 + \overline{\mathbf{r}}_7 + \overline{\mathbf{r}}_8 + \overline{\mathbf{S}}_8 \tag{34}$$

By changing the versors base at crossing from a reference coordinate system to another (introducing the coordinate transformation matrices):

$$\{\overline{\mathbf{r}}_A^{T_{Cx}}\} = \{\mathbf{r}_1\}^T \cdot \{\overline{\mathbf{W}}_{Cx}\} \tag{50}$$

By analyzing (35)- (42) it can be observed that:

$$[A_{Cx2}] = [A_{12}] \cdot [A_{Cx1}] \tag{43}$$

$$[A_{Cx3}] = [A_{23}] \cdot [A_{12}] \cdot [A_{Cx1}] \tag{44}$$

$$[A_{Cx4}] = [A_{34}] \cdot [A_{23}] \cdot [A_{12}] \cdot [A_{Cx1}] = [A_{34}] \cdot [A_{Cx3}] \tag{45}$$

$$[A_{Cx5}] = [A_{45}] \cdot [A_{34}] \cdot [A_{23}] \cdot [A_{12}] \cdot [A_{Cx1}] = [A_{45}] \cdot [A_{Cx4}] \tag{46}$$

$$[A_{Cx6}] = [A_{56}] \cdot [A_{45}] \cdot [A_{34}] \cdot [A_{23}] \cdot [A_{12}] \cdot [A_{Cx1}] = [A_{56}] \cdot [A_{Cx5}] \tag{47}$$

$$\begin{aligned}
 [A_{Cx7}] &= [A_{67}] \cdot [A_{56}] \cdot [A_{45}] \cdot [A_{34}] \cdot [A_{23}] \cdot \\
 &\cdot [A_{12}] \cdot [A_{Cx1}] = [A_{67}] \cdot [A_{Cx6}]
 \end{aligned}
 \tag{48}$$

$$\begin{aligned}
 [A_{Cx8}] &= [A_{78}] \cdot [A_{67}] \cdot [A_{56}] \cdot [A_{45}] \cdot [A_{34}] \cdot \\
 &\cdot [A_{23}] \cdot [A_{12}] \cdot [A_{Cx1}] = [A_{78}] \cdot [A_{Cx7}]
 \end{aligned}
 \tag{49}$$

Based on (43)-(49), the coordinates transformation matrices will be identified for each kinematic joints, with $\alpha_{i,i+1} = 90^\circ$, and $i = \overline{1, 8}$.

Points: *A, B, C, D, E, F, G, H and M* positions depending with T_{Cx} coordinate system, bounded to the coxae bone, will be identified through the following:

$$\left\{ \overline{V}_B^{-T_{cx}} \right\} = \{r_1\}^T \cdot \left\{ \overline{W}_{cx} \right\} + \{r_2\}^T \cdot [A_{cx1}] \cdot \left\{ \overline{W}_{cx} \right\} \quad (51)$$

$$\left\{ \overline{V}_C^{-T_{cx}} \right\} = \{r_1\}^T \cdot \left\{ \overline{W}_{cx} \right\} + \{r_2\}^T \cdot [A_{cx1}] \cdot \left\{ \overline{W}_{cx} \right\} + \{r_3\}^T \cdot [A_{12}] \cdot [A_{cx1}] \cdot \left\{ \overline{W}_{cx} \right\} \quad (52)$$

$$\left\{ \overline{V}_D^{-T_{cx}} \right\} = \{r_1\}^T \cdot \left\{ \overline{W}_{cx} \right\} + \{r_2\}^T \cdot [A_{cx1}] \cdot \left\{ \overline{W}_{cx} \right\} + \{r_3\}^T \cdot [A_{12}] \cdot [A_{cx1}] \cdot \left\{ \overline{W}_{cx} \right\} + \{r_4\}^T \cdot [A_{23}] \cdot [A_{12}] \cdot [A_{cx1}] \cdot \left\{ \overline{W}_{cx} \right\} \quad (53)$$

$$\left\{ \overline{V}_E^{-T_{cx}} \right\} = \{r_1\}^T \cdot \left\{ \overline{W}_{cx} \right\} + \{r_2\}^T \cdot [A_{cx1}] \cdot \left\{ \overline{W}_{cx} \right\} + \{r_3\}^T \cdot [A_{12}] \cdot [A_{cx1}] \cdot \left\{ \overline{W}_{cx} \right\} + \{r_4\}^T \cdot [A_{23}] \cdot [A_{12}] \cdot [A_{cx1}] \cdot \left\{ \overline{W}_{cx} \right\} + \{r_5\}^T \cdot [A_{34}] \cdot [A_{23}] \cdot [A_{12}] \cdot [A_{cx1}] \cdot \left\{ \overline{W}_{cx} \right\} \quad (54)$$

$$\left\{ \overline{V}_F^{-T_{cx}} \right\} = \{r_1\}^T \cdot \left\{ \overline{W}_{cx} \right\} + \{r_2\}^T \cdot [A_{cx1}] \cdot \left\{ \overline{W}_{cx} \right\} + \{r_3\}^T \cdot [A_{12}] \cdot [A_{cx1}] \cdot \left\{ \overline{W}_{cx} \right\} + \{r_4\}^T \cdot [A_{23}] \cdot [A_{12}] \cdot [A_{cx1}] \cdot \left\{ \overline{W}_{cx} \right\} + \{r_5\}^T \cdot [A_{34}] \cdot [A_{23}] \cdot [A_{12}] \cdot [A_{cx1}] \cdot \left\{ \overline{W}_{cx} \right\} + \{r_6\}^T \cdot [A_{45}] \cdot [A_{34}] \cdot [A_{23}] \cdot [A_{12}] \cdot [A_{cx1}] \cdot \left\{ \overline{W}_{cx} \right\} \quad (55)$$

$$\left\{ \overline{V}_G^{-T_{cx}} \right\} = \{r_1\}^T \cdot \left\{ \overline{W}_{cx} \right\} + \{r_2\}^T \cdot [A_{cx1}] \cdot \left\{ \overline{W}_{cx} \right\} + \{r_3\}^T \cdot [A_{12}] \cdot [A_{cx1}] \cdot \left\{ \overline{W}_{cx} \right\} + \{r_4\}^T \cdot [A_{23}] \cdot [A_{12}] \cdot [A_{cx1}] \cdot \left\{ \overline{W}_{cx} \right\} + \{r_5\}^T \cdot [A_{34}] \cdot [A_{23}] \cdot [A_{12}] \cdot [A_{cx1}] \cdot \left\{ \overline{W}_{cx} \right\} + \{r_6\}^T \cdot [A_{45}] \cdot [A_{34}] \cdot [A_{23}] \cdot [A_{12}] \cdot [A_{cx1}] \cdot \left\{ \overline{W}_{cx} \right\} + \{r_7\}^T \cdot [A_{56}] \cdot [A_{45}] \cdot [A_{34}] \cdot [A_{23}] \cdot [A_{12}] \cdot [A_{cx1}] \cdot \left\{ \overline{W}_{cx} \right\} \quad (56)$$

$$\left\{ \overline{V}_H^{-T_{cx}} \right\} = \{r_1\}^T \cdot \left\{ \overline{W}_{cx} \right\} + \{r_2\}^T \cdot [A_{cx1}] \cdot \left\{ \overline{W}_{cx} \right\} + \{r_3\}^T \cdot [A_{12}] \cdot [A_{cx1}] \cdot \left\{ \overline{W}_{cx} \right\} + \{r_4\}^T \cdot [A_{23}] \cdot [A_{12}] \cdot [A_{cx1}] \cdot \left\{ \overline{W}_{cx} \right\} + \{r_5\}^T \cdot [A_{34}] \cdot [A_{23}] \cdot [A_{12}] \cdot [A_{cx1}] \cdot \left\{ \overline{W}_{cx} \right\} + \{r_6\}^T \cdot [A_{45}] \cdot [A_{34}] \cdot [A_{23}] \cdot [A_{12}] \cdot [A_{cx1}] \cdot \left\{ \overline{W}_{cx} \right\} + \{r_7\}^T \cdot [A_{56}] \cdot [A_{45}] \cdot [A_{34}] \cdot [A_{23}] \cdot [A_{12}] \cdot [A_{cx1}] \cdot \left\{ \overline{W}_{cx} \right\} + \{r_8\}^T \cdot [A_{67}] \cdot [A_{56}] \cdot [A_{45}] \cdot [A_{34}] \cdot [A_{23}] \cdot [A_{12}] \cdot [A_{cx1}] \cdot \left\{ \overline{W}_{cx} \right\} \quad (57)$$

$$\left\{ \overline{V}_M^{-T_{cx}} \right\} = \{r_1\}^T \cdot \left\{ \overline{W}_{cx} \right\} + \{r_2\}^T \cdot [A_{cx1}] \cdot \left\{ \overline{W}_{cx} \right\} + \{r_3\}^T \cdot [A_{12}] \cdot [A_{cx1}] \cdot \left\{ \overline{W}_{cx} \right\} + \{r_4\}^T \cdot [A_{23}] \cdot [A_{12}] \cdot [A_{cx1}] \cdot \left\{ \overline{W}_{cx} \right\} + \{r_5\}^T \cdot [A_{34}] \cdot [A_{23}] \cdot [A_{12}] \cdot [A_{cx1}] \cdot \left\{ \overline{W}_{cx} \right\} + \{r_6\}^T \cdot [A_{45}] \cdot [A_{34}] \cdot [A_{23}] \cdot [A_{12}] \cdot [A_{cx1}] \cdot \left\{ \overline{W}_{cx} \right\} + \{r_7\}^T \cdot [A_{56}] \cdot [A_{45}] \cdot [A_{34}] \cdot [A_{23}] \cdot [A_{12}] \cdot [A_{cx1}] \cdot \left\{ \overline{W}_{cx} \right\} + \{r_8\}^T \cdot [A_{67}] \cdot [A_{56}] \cdot [A_{45}] \cdot [A_{34}] \cdot [A_{23}] \cdot [A_{12}] \cdot [A_{cx1}] \cdot \left\{ \overline{W}_{cx} \right\} + \{r_9\}^T \cdot [A_{78}] \cdot [A_{67}] \cdot [A_{56}] \cdot [A_{45}] \cdot [A_{34}] \cdot [A_{23}] \cdot [A_{12}] \cdot [A_{cx1}] \cdot \left\{ \overline{W}_{cx} \right\} \quad (58)$$

B. Velocities Analysis

The research aim is to determine the “M” point velocity depending on T_{cx} reference system. Firstly the (50)-(51) mathematical expressions will be differentiated, but for achieving the main purpose it is necessary to create the non symmetric matrices for each joint, like this form:

$$\left[\begin{matrix} \tilde{\omega}_{Cxi} \end{matrix} \right] = \begin{bmatrix} 0 & \omega_{Cxi} & -\omega_{Cxi} \\ -\omega_{Cxi} & 0 & \omega_{Cxi} \\ \omega_{Cxi} & -\omega_{Cxi} & 0 \end{bmatrix}, \text{ with } i, j = \overline{1,8} \quad (59)$$

For this:

$$\left[\dot{A}_{Cx1} \right] = \left[\tilde{\omega}_{Cx1} \right] \cdot \left[A_{Cx1} \right] \quad (60)$$

$$\left[\dot{A}_{Cx2} \right] = \left[\tilde{\omega}_{12} \right] \cdot \left[A_{Cx3} \right] \quad (61)$$

$$\left[\dot{A}_{Cx3} \right] = \left[\tilde{\omega}_{23} \right] \cdot \left[A_{Cx3} \right] \quad (62)$$

$$\left[\dot{A}_{Cx4} \right] = \left[\tilde{\omega}_{34} \right] \cdot \left[A_{Cx4} \right] \quad (63)$$

$$\left[\dot{A}_{Cx5} \right] = \left[\tilde{\omega}_{45} \right] \cdot \left[A_{Cx5} \right] \quad (64)$$

$$\left[\dot{A}_{Cx6} \right] = \left[\tilde{\omega}_{56} \right] \cdot \left[A_{Cx7} \right] \quad (65)$$

$$\left[\dot{A}_{Cx7} \right] = \left[\tilde{\omega}_{67} \right] \cdot \left[A_{Cx7} \right] \quad (66)$$

$$\left[\dot{A}_{Cx8} \right] = \left[\tilde{\omega}_{78} \right] \cdot \left[A_{Cx8} \right] \quad (67)$$

For each “A, B, C, D, E, F, G, H” and “M” points will be obtained:

$$\left\{ \overline{V}_A^{-T_{cx}} \right\} = 0 \quad (68)$$

$$\left\{ \overline{V}_B^{-T_{cx}} \right\} = 0 + \{r_2\}^T \cdot \left[\tilde{\omega}_{Cx1} \right] \cdot [A_{Cx1}] \cdot \left\{ \overline{W}_{cx} \right\} \quad (69)$$

$$\left\{ \overline{V}_C^{-T_{cx}} \right\} = 0 + \{r_2\}^T \cdot \left[\tilde{\omega}_{Cx1} \right] \cdot [A_{Cx1}] \cdot \left\{ \overline{W}_{cx} \right\} + \{r_3\}^T \cdot \left[\tilde{\omega}_{12} \right] \cdot [A_{Cx2}] \cdot \left\{ \overline{W}_{cx} \right\} \quad (70)$$

$$\begin{aligned} \{\bar{v}_D^{-Tex}\} &= 0 + \{r_2\}^T \cdot \left[\tilde{\omega}_{cx1} \right] \cdot [A_{Cx1}] \cdot \{\bar{w}_{cx}\} + \\ &+ \{r_3\}^T \cdot \left[\tilde{\omega}_{12} \right] \cdot [A_{Cx2}] \cdot \{\bar{w}_{cx}\} + \\ &+ \{r_4\}^T \cdot \left[\tilde{\omega}_{23} \right] \cdot [A_{Cx3}] \cdot \{\bar{w}_{cx}\} \end{aligned} \tag{71}$$

$$\begin{aligned} \{\bar{v}_E^{-Tex}\} &= 0 + \{r_2\}^T \cdot \left[\tilde{\omega}_{cx1} \right] \cdot [A_{Cx1}] \cdot \{\bar{w}_{cx}\} + \\ &+ \{r_3\}^T \cdot \left[\tilde{\omega}_{12} \right] \cdot [A_{Cx2}] \cdot \{\bar{w}_{cx}\} + \{r_4\}^T \cdot \left[\tilde{\omega}_{23} \right] \cdot \\ &\cdot [A_{Cx3}] \cdot \{\bar{w}_{cx}\} + \{r_5\}^T \cdot \left[\tilde{\omega}_{34} \right] \cdot [A_{Cx4}] \cdot \{\bar{w}_{cx}\} \end{aligned} \tag{72}$$

$$\begin{aligned} \{\bar{v}_F^{-Tex}\} &= 0 + \{r_2\}^T \cdot \left[\tilde{\omega}_{cx1} \right] \cdot [A_{Cx1}] \cdot \{\bar{w}_{cx}\} + \\ &+ \{r_3\}^T \cdot \left[\tilde{\omega}_{12} \right] \cdot [A_{Cx2}] \cdot \{\bar{w}_{cx}\} + \{r_4\}^T \cdot \left[\tilde{\omega}_{23} \right] \cdot \\ &\cdot [A_{Cx3}] \cdot \{\bar{w}_{cx}\} + \{r_5\}^T \cdot \left[\tilde{\omega}_{34} \right] \cdot [A_{Cx4}] \cdot \{\bar{w}_{cx}\} + \\ &+ \{r_6\}^T \cdot \left[\tilde{\omega}_{45} \right] \cdot [A_{Cx5}] \cdot \{\bar{w}_{cx}\} \end{aligned} \tag{73}$$

$$\begin{aligned} \{\bar{v}_G^{-Tex}\} &= 0 + \{r_2\}^T \cdot \left[\tilde{\omega}_{cx1} \right] \cdot [A_{Cx1}] \cdot \{\bar{w}_{cx}\} + \\ &+ \{r_3\}^T \cdot \left[\tilde{\omega}_{12} \right] \cdot [A_{Cx2}] \cdot \{\bar{w}_{cx}\} + \{r_4\}^T \cdot \left[\tilde{\omega}_{23} \right] \cdot [A_{Cx3}] \cdot \\ &\cdot \{\bar{w}_{cx}\} + \{r_5\}^T \cdot \left[\tilde{\omega}_{34} \right] \cdot [A_{Cx4}] \cdot \{\bar{w}_{cx}\} + \{r_6\}^T \cdot \left[\tilde{\omega}_{45} \right] \cdot \\ &\cdot [A_{Cx5}] \cdot \{\bar{w}_{cx}\} + \{r_7\}^T \cdot \left[\tilde{\omega}_{56} \right] \cdot [A_{Cx6}] \cdot \{\bar{w}_{cx}\} \end{aligned} \tag{74}$$

$$\begin{aligned} \{\bar{v}_H^{-Tex}\} &= 0 + \{r_2\}^T \cdot \left[\tilde{\omega}_{cx1} \right] \cdot [A_{Cx1}] \cdot \{\bar{w}_{cx}\} + \\ &+ \{r_3\}^T \cdot \left[\tilde{\omega}_{12} \right] \cdot [A_{Cx2}] \cdot \{\bar{w}_{cx}\} + \{r_4\}^T \cdot \left[\tilde{\omega}_{23} \right] \cdot \\ &\cdot [A_{Cx3}] \cdot \{\bar{w}_{cx}\} + \{r_5\}^T \cdot \left[\tilde{\omega}_{34} \right] \cdot [A_{Cx4}] \cdot \{\bar{w}_{cx}\} + \\ &+ \{r_6\}^T \cdot \left[\tilde{\omega}_{45} \right] \cdot [A_{Cx5}] \cdot \{\bar{w}_{cx}\} + \{r_7\}^T \cdot \left[\tilde{\omega}_{56} \right] \cdot \\ &\cdot [A_{Cx6}] \cdot \{\bar{w}_{cx}\} + \{r_8\}^T \cdot \left[\tilde{\omega}_{67} \right] \cdot [A_{Cx7}] \cdot \{\bar{w}_{cx}\} \end{aligned} \tag{75}$$

$$\begin{aligned} \{\bar{v}_M^{-Tex}\} &= 0 + \{r_2\}^T \cdot \left[\tilde{\omega}_{cx1} \right] \cdot [A_{Cx1}] \cdot \{\bar{w}_{cx}\} + \\ &+ \{r_3\}^T \cdot \left[\tilde{\omega}_{12} \right] \cdot [A_{Cx2}] \cdot \{\bar{w}_{cx}\} + \{r_4\}^T \cdot \left[\tilde{\omega}_{23} \right] \cdot \\ &\cdot [A_{Cx3}] \cdot \{\bar{w}_{cx}\} + \{r_5\}^T \cdot \left[\tilde{\omega}_{34} \right] \cdot [A_{Cx4}] \cdot \{\bar{w}_{cx}\} + \\ &+ \{r_6\}^T \cdot \left[\tilde{\omega}_{45} \right] \cdot [A_{Cx5}] \cdot \{\bar{w}_{cx}\} + \{r_7\}^T \cdot \left[\tilde{\omega}_{56} \right] \cdot \\ &\cdot [A_{Cx6}] \cdot \{\bar{w}_{cx}\} + \{r_8\}^T \cdot \left[\tilde{\omega}_{67} \right] \cdot [A_{Cx7}] \cdot \{\bar{w}_{cx}\} + \\ &+ \{S_8\}^T \cdot \left[\tilde{\omega}_{78} \right] \cdot [A_{Cx8}] \cdot \{\bar{w}_{cx}\} \end{aligned} \tag{76}$$

C. Accelerations Analysis

Accelerations mathematical expressions will be obtained by differentiating (68)-(76) successively. For “A”, and “B” joints, the accelerations from (77) and (78) will be obtained.

$$\{\bar{a}_A^{-Tex}\} = 0 \tag{77}$$

$$\begin{aligned} \{\bar{a}_B^{-Tex}\} &= 0 + \{r_2\}^T \cdot \left[\dot{\tilde{\omega}}_{cx1} \right] \cdot [A_{Cx1}] \cdot \{\bar{w}_{cx}\} + \\ &+ \{r_2\}^T \cdot \left[\tilde{\omega}_{cx1} \right] \cdot \left[\dot{\tilde{\omega}}_{cx1} \right] \cdot [A_{Cx1}] \cdot \{\bar{w}_{cx}\} \end{aligned} \tag{78}$$

Similarly, the accelerations of the “C, D, E, F, G, H”, points will be obtained. The acceleration of “M” point is given by (79):

$$\begin{aligned} \{\bar{a}_M^{-Tex}\} &= 0 + \{r_2\}^T \cdot \left[\dot{\tilde{\omega}}_{cx1} \right] \cdot [A_{Cx1}] \cdot \{\bar{w}_{cx}\} + \{r_2\}^T \cdot \left[\tilde{\omega}_{cx1} \right] \cdot \\ &\cdot \left[\dot{\tilde{\omega}}_{cx1} \right] \cdot [A_{Cx1}] \cdot \{\bar{w}_{cx}\} + \{r_3\}^T \cdot \left[\dot{\tilde{\omega}}_{12} \right] \cdot [A_{Cx2}] \cdot \{\bar{w}_{cx}\} + \\ &+ \{r_3\}^T \cdot \left[\tilde{\omega}_{12} \right] \cdot \left[\dot{\tilde{\omega}}_{12} \right] \cdot [A_{Cx2}] \cdot \{\bar{w}_{cx}\} + \{r_4\}^T \cdot \left[\dot{\tilde{\omega}}_{23} \right] \cdot \\ &\cdot [A_{Cx3}] \cdot \{\bar{w}_{cx}\} + \{r_4\}^T \cdot \left[\tilde{\omega}_{23} \right] \cdot \left[\dot{\tilde{\omega}}_{23} \right] \cdot [A_{Cx3}] \cdot \{\bar{w}_{cx}\} + \\ &+ \{r_5\}^T \cdot \left[\dot{\tilde{\omega}}_{34} \right] \cdot [A_{Cx4}] \cdot \{\bar{w}_{cx}\} + \{r_5\}^T \cdot \left[\tilde{\omega}_{34} \right] \cdot \left[\dot{\tilde{\omega}}_{34} \right] \cdot \\ &\cdot [A_{Cx4}] \cdot \{\bar{w}_{cx}\} + \{r_6\}^T \cdot \left[\dot{\tilde{\omega}}_{45} \right] \cdot [A_{Cx5}] \cdot \{\bar{w}_{cx}\} + \\ &+ \{r_6\}^T \cdot \left[\tilde{\omega}_{45} \right] \cdot \left[\dot{\tilde{\omega}}_{45} \right] \cdot [A_{Cx5}] \cdot \{\bar{w}_{cx}\} + \{r_7\}^T \cdot \left[\dot{\tilde{\omega}}_{56} \right] \cdot [A_{Cx6}] \cdot \{\bar{w}_{cx}\} + \\ &+ \{r_7\}^T \cdot \left[\tilde{\omega}_{56} \right] \cdot \left[\dot{\tilde{\omega}}_{56} \right] \cdot [A_{Cx6}] \cdot \{\bar{w}_{cx}\} + \{r_8\}^T \cdot \left[\dot{\tilde{\omega}}_{67} \right] \cdot [A_{Cx7}] \cdot \{\bar{w}_{cx}\} + \\ &+ \{r_8\}^T \cdot \left[\tilde{\omega}_{67} \right] \cdot \left[\dot{\tilde{\omega}}_{67} \right] \cdot [A_{Cx7}] \cdot \{\bar{w}_{cx}\} + \{S_8\}^T \cdot \left[\dot{\tilde{\omega}}_{78} \right] \cdot [A_{Cx8}] \cdot \{\bar{w}_{cx}\} + \\ &\{S_8\}^T \cdot \left[\tilde{\omega}_{78} \right] \cdot \left[\dot{\tilde{\omega}}_{78} \right] \cdot [A_{Cx8}] \cdot \{\bar{w}_{cx}\} \end{aligned} \tag{79}$$

IV. NUMERICAL PROCESSING

By considering the kinematic model from Fig. 2, a parameterized one will be processed with the aid of MAPLE software by inserting the above algorithm and considering known the geometrical elements. Thus, the geometrical elements dimensions are: $L_{cx}=137.5$ millimeters; $L_1=9$ millimeters; $L_2=9$ millimeters; $L_3=275$ millimeters; $L_4=2.5$ millimeters; $L_5=260$ millimeters; $L_6=9$ millimeters; $L_7=31.85$

millimeters; $L_8=50.42$ millimeters. This corresponds to a child with an age of 7 years old.

The time parameter was introduced as 1.4 seconds and corresponds to a 100% complete gait.

The generalized coordinate system variations in case of the analyzed joints equivalent to the human lower limb are shown in Figs. 3-6.

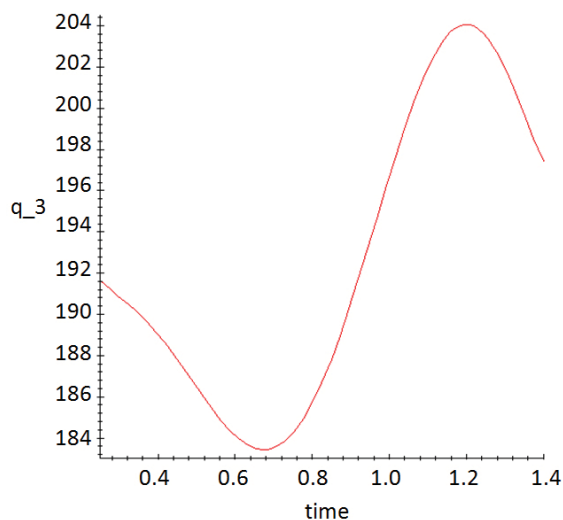


Fig. 3 Processed “q3” variation angle [degrees], corresponding with the equivalent hip joint vs. time [seconds]

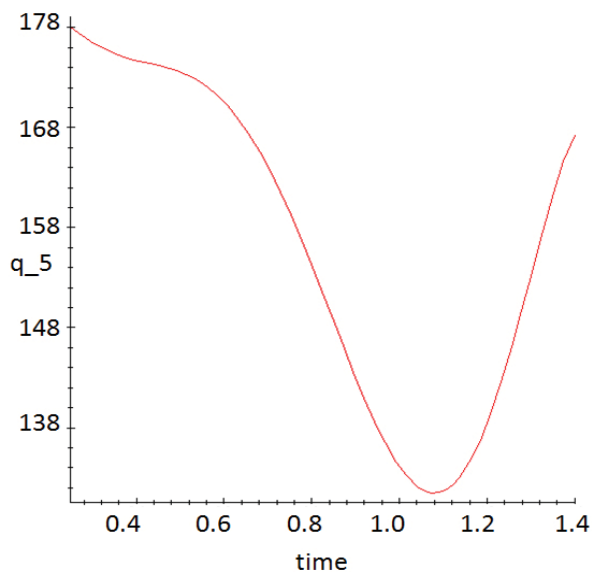


Fig. 4 Processed “q5” variation angle [degrees], corresponding with the equivalent knee joint vs. time [seconds]

By creating a parameterized simplified model of the one from Fig. 2 using SolidWorks software, the obtained motion laws from Figs. 3-6 were used as input data for a virtual simulation. This model is presented in Fig. 7. In this way, the obtained kinematic results were validated.

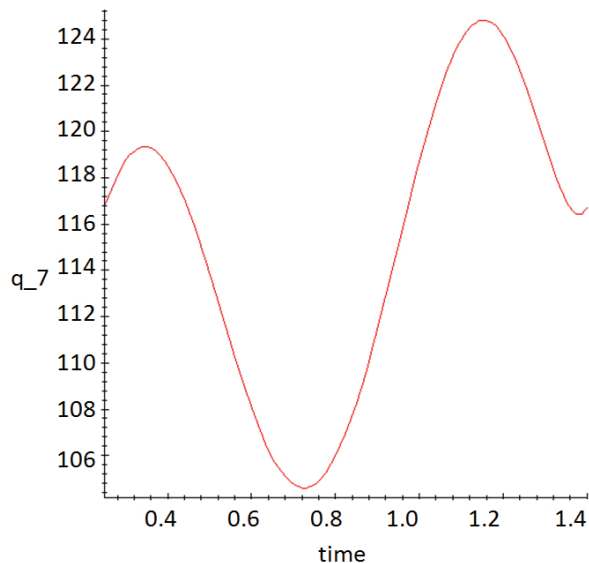


Fig. 5 Processed “q7” variation angle [degrees], corresponding with the equivalent ankle joint vs. time [seconds]

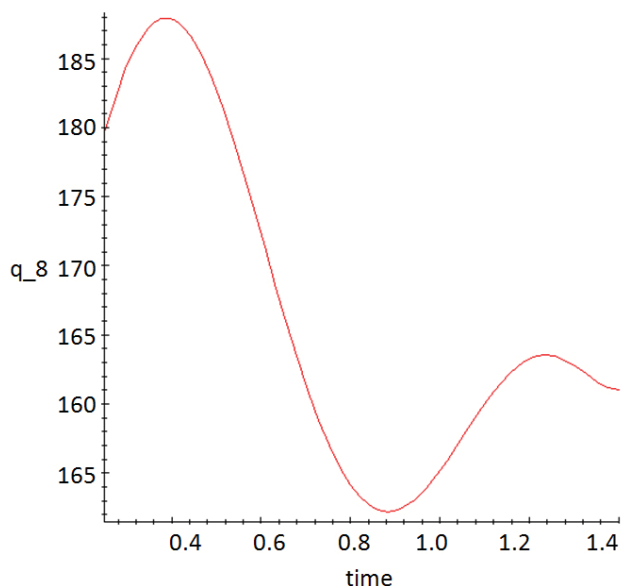


Fig. 6 Processed “q8” variation angle [degrees], corresponding with the equivalent foot joint vs. time [seconds]

The essential input data for further research is represented by the “q5” variation angle, which this corresponds for the child knee motion laws. It can be observed that this develops angular amplitude of 40 degrees and by referring to [12] this is a reasonable and true result. Thus, this motion law will serve as input data for the new knee modular orthosis virtual simulations and prototype validation.

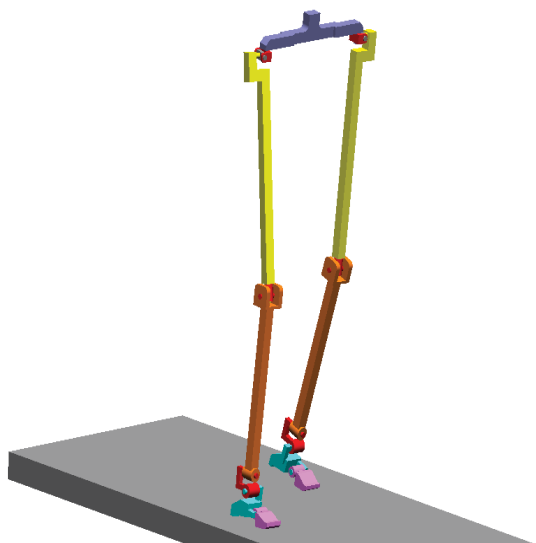


Fig. 7 A simplified virtual model, designed and simulated with SolidWorks

V.KINEMATIC RESULTS APPLICATION ONTO NEW KNEE MODULAR ORTHOSIS

A. Child Knee Modular Orthosis

Specific kinetotherapeutic procedures consist only in flexion/extension exercises in order to emphasize the traumatized knee joint angular amplitude. For these, an orthosis modular structure was designed in order to add or remove modules for increasing or decreasing the size of this. The structural model is shown in Fig. 8, and from this, a virtual model designed in SolidWorks. This is shown in Fig. 9.

In reality, for the modular orthosis' command and control a servomotor will be used, and an Arduino microcontroller board.

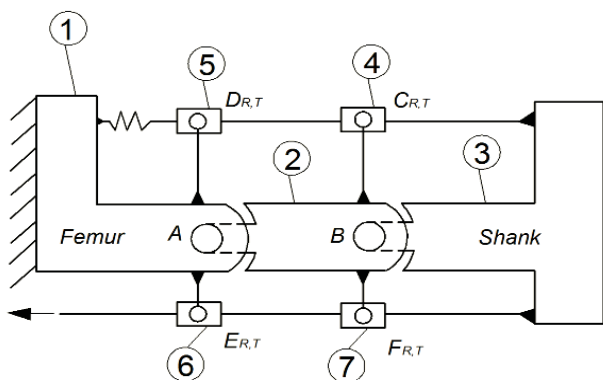


Fig. 8 A structural scheme of the proposed knee modular orthosis

The link between the command-control unit and the modular orthosis will be made through flexible cables, one for pull up – cable no: 1 and the other for roll back – cable no: 2.

The virtual model was imported in MSC ADAMS, AdamsView module based on an interface between SolidWorks and this software [13]. The material which will be

used for components is aluminum alloys. For simulations, the right limb motion law from Fig. 4 was applied on the Cable no.1 (Fig. 8).

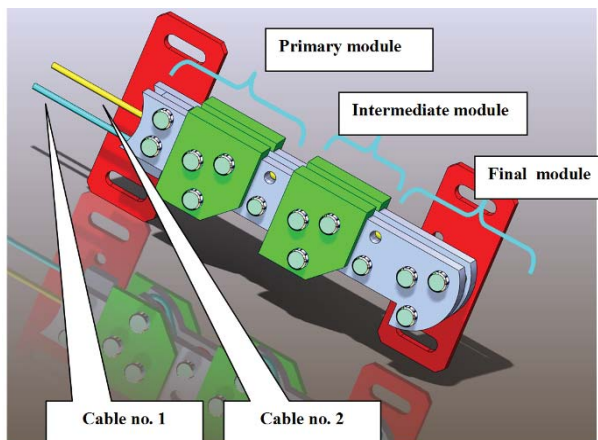


Fig. 9 CAD model of the proposed knee modular orthosis designed on SolidWorks

The femur component of primary module was fixed and a load force equal with 470 Newton [8] was applied on final module (this force was determined in a previous work of the authors according with literature data). This force is equivalent with the child's weight. The actuating cables were designed and simulated as flexible ones.

After a complete virtual simulation as it can be seen in Fig. 10, the final module angular motion value was 38.7 degrees. This result is represented in Fig. 11 and validates the functional and structural principle of the proposed knee orthosis.

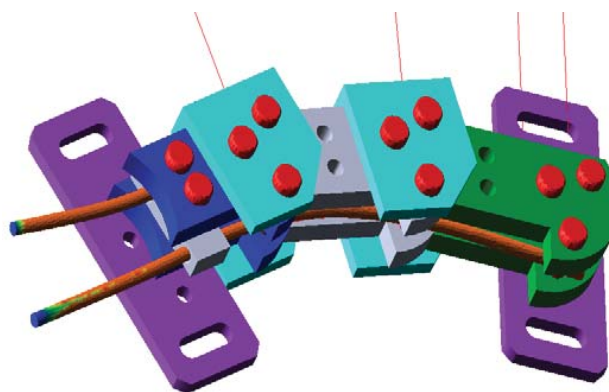


Fig. 10 Snapshot obtained during virtual simulations of the proposed knee modular orthosis

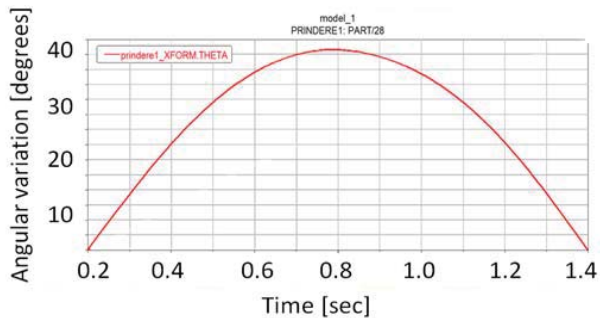


Fig. 11 Knee modular orthosis angular variation during a simulation

VI. KNEE MODULAR ORTHOSIS PROTOTYPE AND REAL TESTS

The proposed virtual model leads to 2D drawings of each element and these can be useful for manufacturing operations. In this way, a prototype was fabricated and this is shown in Fig. 12.

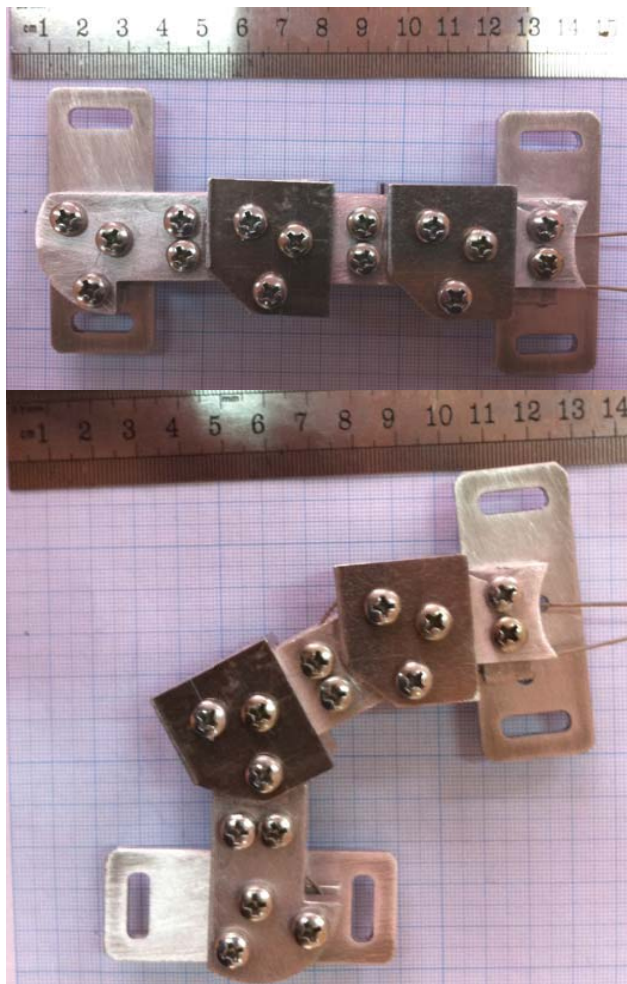


Fig. 12 Knee modular orthosis prototype

As it was affirmed on the above research section, the command and control was designed by using ARDUINO

board and a servomotor unit for actuating this. A snapshot of this is represented in Fig. 13.

In order to validate the modular orthosis prototype, a 7 years old child with locomotion disability will perform flexion/extension exercises and the motion laws will be achieved with CONTEMPLAS High Speed Motion Analysis equipment (Machine Elements laboratory - Faculty of Mechanics, University of Craiova). This child has a trauma at the right shank's level, and also the knee joint was affected. The prototype is presented in Fig. 14, during experimental tests.

As a template from a database developed in this way, for a healthy 7 years old child the knee angular amplitude for a single gait is represented in Fig. 15. The knee angular amplitude developed by a healthy child for walking was 39.2 degrees, and in the knee modular orthosis case was 43 degrees.



Fig. 13 Knee modular orthosis prototype with attached command&control unit



Fig. 14 A 7 years old child with the developed knee modular orthosis prototype

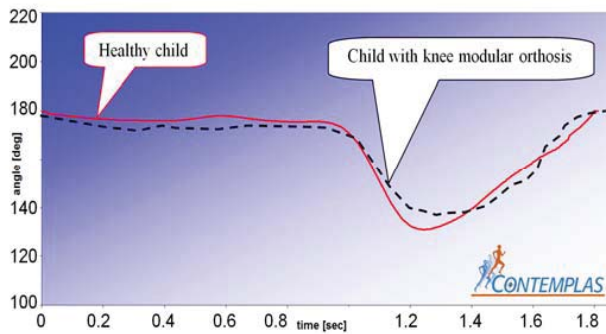


Fig. 15 Comparison between the experimental motion law of the developed knee modular orthosis prototype and a healthy child

VII. CONCLUSIONS

This research validates a modular knee orthosis type based on kinematic considerations. Novel elements brought by this research are:

- A modern kinematic method for computing joints motion law;
- Developing an interface in order to transfer the virtual model from SolidWorks software, to MSC ADAMS;
- Modern equipments were used for evaluating the human subjects;
- A modular orthosis design which can be adapted on children legs for knee joint rehabilitation in walking. This can be modified by adding or removing modules.

The elaborated prototype can be used on further medical application, specific to a specialist from neuromotor rehabilitation field, helping him to develop rehabilitation programs especially dedicated for children lower limbs.

By taking out elements from the knee orthosis, this can be readapted to a child knee with an age lower than 7 years. Thus, by considering the system gait and posture rehabilitation, through this modular knee orthosis prototype it can be included specific muscle training, balance training and coordination. Gait and posture rehabilitation can be assessed by a video motion analysis equipment and after this it can be created individual models of modular orthoses. These can easily simplify the lower limb rehabilitation especially in case of a child due to the same specific rehabilitation techniques used in case of an adult. This includes the muscle groups that are involved in devices function.

The final conclusion stands on the mathematical model from the kinematic analysis, which helps to increase the results of gait and posture rehabilitation by bringing a major advantage to the locomotion system function.

REFERENCES

- [1] B. Weinberg, S. Patel, et al., "Design, Control and Human Testing of an Active Knee Rehabilitation Orthotic Device", in *2007 IEEE International Conference on Robotics and Automation*, pp. 4126-4133.
- [2] J. A. Blaya, H. Herr, "Adaptive Control of a Variable-Impedance Ankle-Foot Orthosis to Assist Drop-Foot Gait", *IEEE Trans Neural Syst Rehabil Eng*, 12(1), pp. 24-31, 2004.
- [3] K. Koyanagi, J. Furusho, U. Ryu A. Inoue, "Development of Rehabilitation System for the Upper Limbs in a NEDO Project,"

Proceedings - 2003, IEEE International Conference on Robotics and Automation, Vol. 3, pp. 4016-4022.

- [4] J.D. Carlson, W. Matthis, J.R. Toscano, "Smart Prosthetics Based on Magnetorheological Fluids," in *Proceedings of SPIE - The International Society for Optical Engineering*, 2001, Vol. 4332, pp. 308-316.
- [5] S. Dong, K. Lu, J.Q. Sun, K. Rudolph, "Rehabilitation Device with Variable Resistance and Intelligent Control", in *Medical Engineering and Physics*, Vol. 27, No. 3, 2005, pp. 249-255.
- [6] C. Copilusi, N. Dumitru, M. Marin, L. Rusu, "Children Orthotics and Prostheses Devices Designed from Cinematic and Dynamic Considerations", *Engineering Letters Journal*. Vol. 20:4. pp. 301-316. 2012.
- [7] Ma Hao and Wei-Hsin Liao, "Design optimization of a magnetorheological brake in powered knee orthosis", *Proc. SPIE 9431, Active and Passive Smart Structures and Integrated Systems*. 2015.
- [8] C. Copilusi, "Researches regarding some mechanical systems applicable in medicine". PhD. Thesis, Faculty of Mechanics, Craiova. 2009.
- [9] A. Heyn, R. E. Mayagoitia, A. V. Nene, and P. H. Veltink, "The kinematics of the swing phase obtained from accelerometer and gyroscope measurements", in: *Proceedings of the 18th Int. Conf. IEEE Engineering in Medicine and Biology Society—Bridging Disciplines for Biomedicine*, pp. 463-464. 1996.
- [10] D. Hooman, M. Brigitte, et al., "Estimation and Visualization of Sagittal Kinematics of Lower Limbs Orientation Using Body-Fixed Sensors", in: *IEEE Transactions on Biomedical Engineering*, Vol. 53, No. 7, pp. 1385-1393. 2006.
- [11] R. M. Kiss, L. Kocsis, and Z. Knoll, "Joint kinematics and spatial temporal parameters of gait measured by an ultrasound-based system", in: *Med. Eng. Phys. Journal*, vol. 26, pp. 611-620. 2004.
- [12] M. Williams, "Biomechanics of human motion". W.B. Saunders Co. Philadelphia and Lon-don, U.K. 1996.
- [13] J. Giesbers, "Contact Mechanics in MSC Adams. A technical evaluation of the contact models in multibody dynamics software MSC Adams". Bachelor Thesis. University of Twente. 2012.